Progress In Electromagnetics Research M, Vol. 44, 31–38, 2015

Discriminating the Frequency Dispersive Scattering Centres of Complex Targets by Wideband Group Delay Analysis

Hamid Heidar and Rahman Sofiani*

Abstract—Waveguide geometry is one of the most critical frequency Dispersive Scattering Centres (DSCs) in actual complex radar targets. Because of the occurrence of nonlinear dispersive scattering phase or range extension phenomena the nearby scatterers may be hidden in such cases. So, degradation of spatial resolution occurs in corresponding range profiles. According to a relatively simple parametric scattering model, a computationally efficient technique is introduced to analyze the complex range profiles including both backscattering field intensity and phase. The group delay of each scatterer is used as a criterion for discriminating the dispersive and non-dispersive ones. The wideband measured data samples are used for evaluating the technique, and the comparison is performed relative to Fourier-based results.

1. INTRODUCTION

The high frequency backscattering response of a complex target emanates from some specific geometrical discontinuities, i.e., phase centres. Hence the total far field seems to be originated from these discrete radiation sources called scattering centres. Commonly, the location of these sources is assumed to be frequency independent. In this case, the wave propagation velocity is also frequency-independent yielding non-dispersive scattering centres. It means that no phase centre shift is expected in a specific bandwidth required in range profile analysis. However, it is not true for waveguides with rigorous dispersive behaviour due to wave penetration inside, yielding significant phase centre shift. The effect of phase centre shift is widening the scatterer radar range profile, i.e., range extension. It is an undesired effect that may cover neighbour scatterers. Hence deterioration happens in spatial resolution of 1-D range profiles or smudge effect in 2-D radar images. Parametric scattering centre modelling is an efficient approach in complicated inverse scattering problems, if suitable basis functions are employed [1–3]. Usually super-resolution techniques are used to determine the unknown parameters.

Hurst and Mittra used an exponential function with slow frequency dependency [4]. This model only assumes the specular reflections from scattering centres and uses PRONY algorithm to determine the model parameters. Potter et al. used a Geometrical Theory of Diffraction (GTD) based frequency dependency [5]. This model introduces a suitable representation for some common diffractive geometries and maximum likelihood algorithm is used to compute the parameters. Trintinalia and Ling modelled dispersive behaviour of a circular waveguide structures through an ESPRIT algorithm [6]. McClure et al. proposed a model to express the dispersion due to creeping waves around the cylindrical structures utilizing Matrix Pencil Method (MPM) [7]. Heidar and Tavakoli developed an enhanced parametric model for analyzing the highly dispersive waveguide scattering centres [8]. In this model, named Enhanced Dispersive Scattering Model (EDSC), a combination of super-resolution PRONY technique and population based Genetic Algorithm (GA) with an intelligent initialization procedure is used to determine the unknown parameters. DSCs appear in actual complex targets scattering response

Received 1 July 2015, Accepted 22 September 2015, Scheduled 6 October 2015
* Corresponding author: Rahman Sofiani (rahman.sofiani@gmail.com).
The authors are with the Electrical & Electronics Department, Malek-Ashtar University of Technology, Tehran, Iran.

like aircrafts having inlet/outlet exhaust. These waveguide geometries are dominant contributors in scattering cross section of the overall target. They may cover wide range of aspect angles with respect to the symmetrical axis of aperture when practical radar illuminates them.

Assuming that the surface resistivity is negligible in actual aerial target, a simpler version of EDSC model is developed in this paper. This model is useful for group delay analysis in complex targets including at least one DSC. Group delay concept in high frequency regime is introduced in Section 2. The jointed scatterers in a waveguide DSC are modelled in Section 3. The group delay analysis to discriminate different scatterers using experimental data is demonstrated in Section 4. The conclusion is given in Section 5.

2. GROUP DELAY CONCEPT

Consider the geometry shown in Figure 1 consisting of a dispersive open ended waveguide passing through a non-dispersive flat plate. Although this geometry is simple, its scattering response is representative for signatures of actual complex targets consisting both dispersive and non-dispersive contributions. The combination of a conducting strip with cavity and fin is used in some references for super-resolution time-frequency analysis of wideband backscattered data [9].

Three independent components are predicted in the scattering response. First: waveguide backscattering response E_s^{wgd} that is considered as the dispersive component. The rim and flat plate responses described by E_s^{rim} and E_s^{plt} account to be non-dispersive components.

Here the front open aperture is excited at small elevation angle θ. So the response of the external surface may be included in E_s^{plt}, and it is assumed to be non-dispersive. However, for perpendicular excitation corresponding to side-looking view ($\theta = 90^\circ$), the creeping wave components may appear to show specific frequency dispersion. Here, the focus is on the frequency dispersion, and the angular variables are not considered in the scattering centre model. However, elevation and azimuth angular dependency is possible to be considered effortlessly [10].

For every arbitrary complex target assuming isotropic point scatterers and omitting $e^{j\omega t}$, the high frequency backscattered far-field is

$$E_s(k,r) = \sum_{m=1}^{\infty} B_m(k,r) e^{-j2kr_m} \tag{1}$$

where k is the free space wave number and r_m the down range of the mth scattering centre along the radar line of sight (LOS). It is proportional to the round-trip free space propagation delay time equal to $2r_m/c$, and c is the free space propagation velocity. B_m is the complex weighting coefficient corresponding to scattering amplitude of each scattering centre. In an ideal point scatter model, the aforementioned complex exponential basis functions have frequency independent weighting coefficients.

In waveguides, as inherently non-point dispersive scattering centres, the phase velocity is frequency dependent, and its effect should be used in modelling procedure. In other words, except the rim and outer flat plate, the backscattering field of the aperture itself experiences frequency dispersion effect. Here, such an independent nonpoint dispersive scattering centre (DSC) is considered as an ensemble of some equivalent point scatterers with an identical frequency dependent correction multiplicand $\xi_m(k)$. In current study, it is called dispersion factor (DF). Various geometries have different DFs. Thus

$$B_m(k,r) = a_m(r)\xi_m(k) = a_m(r)\rho_m(k)e^{-j\varphi_m(k)} \tag{2}$$

where $\rho_m(k)$ and $a_m(r)$ are the frequency dependent and range dependent parts of complex weighting coefficients, respectively. Here $\varphi_m(k)$ appears as the deviation from the linear phase encountered in dispersive media. It is shown that this function has important information to characterize the dispersive nature of scattering centres. Hence, considering M individual scattering centres and focusing on the frequency dispersion, scatter model (1) becomes

$$\begin{aligned} E_s(k) &= \sum_{m=1}^{M} A_m(k) e^{-j\Psi_m(k)} \\ A_m(k) &= a_m\rho_m(k); \quad \Psi_m(k) = 2kr_m + \phi_m(k) \end{aligned} \tag{3}$$

In Eq. (3), $\Psi_m(k)$ and $A_m(k)$ represent the frequency dependent total nonlinear phase and total complex scattering amplitude, respectively. For an arbitrary complex target consisting of merely non-dispersive scattering centres or no frequency dependency, we have $B_m(k,r) = a_m(r)$. Hence, Eq. (3) reduces to the well-defined ideal point scatter model. The overall topic of the above scattering model is described in detail in [8].

The open-ended waveguide duct in Figure 1 acts as a DSC. In such geometries and for the mth equivalent scattering centre, a corresponding nonlinear group delay is defined as the derivative of the backscatter field phase

$$\tau_{dm}^{nl}(k) = -\frac{1}{c}\frac{\partial \Psi_m(k)}{\partial k} = \tau_{dm}^{c} + \tau_{dm}^{dev}(k)\,(\text{sec}) \tag{4}$$

where $\tau_{dm}^{c} = -2r_m/c$ describes the radar test range as a frequency independent term. The second term $\tau_{dm}^{dev} = -(\partial\varphi_m(k)/\partial k)/c$ represents the group delay deviation due to the scattering phase nonlinearity. The latter is known as the source of radar range extension and it is studied for waveguide geometries in [11].

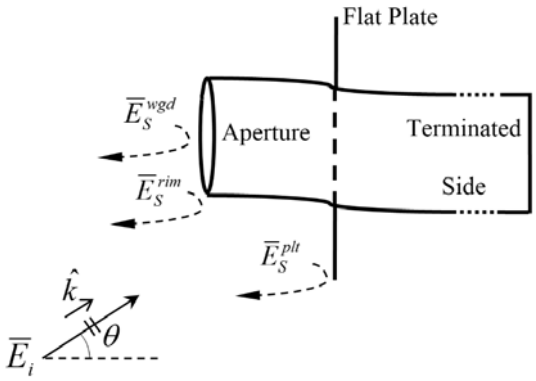

Figure 1. Geometry of the open ended waveguide passing through a flat plate as a complex target excited by a plane wave.

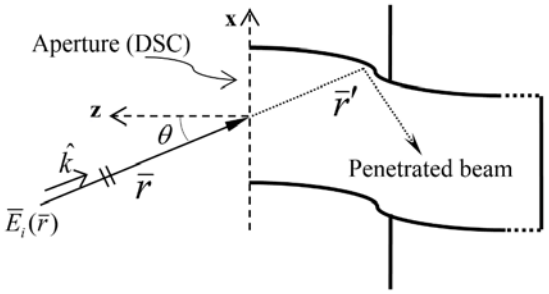

Figure 2. EM wave penetration through the waveguide in small aspect angle yielding the dispersive scattering response.

3. WAVEGUIDE DISPERSIVE SCATTERING CENTRE

At this stage we focus on the waveguide component of the backscattering response. Due to wave penetration and the resulted frequency dispersion, it may appear as a DSC in corresponding radar range profile. As shown in Figure 2, a plane wave of amplitude E_0 illuminates the aperture at a small elevation aspect angle θ.

The radar range in free space as a non-dispersive propagation medium is denoted by r. However, radar range in waveguide as a dispersive propagation medium is indicated by r'. The round trip propagation inside the waveguide makes dominant contribution to the total backscattered field [12]. At the aperture, this component is represented approximately by

$$\hat{E}_s^{wgd}(k,r') \approx \Gamma(r')E_0 e^{-2\gamma(k)r'} = \Gamma(r')E_0 e^{-2\alpha(k)r'} \tag{5}$$

where $\Gamma(r')$ is the waveguide reflection coefficient and $\gamma(k)$ the complex frequency dependent propagation constant. Assuming a symmetrical cross-section, as it is common in most man-made targets, the phase function $\beta(k)$ can be approximated by

$$\beta(k) \approx \sqrt{k^2 - k_c^2}; \quad k > k_c \tag{6}$$

where k_c is the cut-off frequency. Below cut-off frequencies, $k \le k_c$, and backscattering arises only from the edges and the outer surface.

Attenuation in a waveguide is caused by either filled dielectric (if it exists) loss or conductor walls loss. If α_c and α_d are the attenuation constants due to dielectric and conductor losses, respectively, then the total attenuation damping function versus frequency is

$$\alpha(k) = \alpha_d(k) + \alpha_c(k) \tag{7}$$

Simply in an air filled waveguide of finite length α_d can be neglected. The conductor loss depends on the field distribution and it must be evaluated for various waveguides. The attenuation constant due to imperfect conducting walls in both TE and TM modes has identical mathematical representations. For example, considering TE_{10} we have [13]

$$\alpha_c(k) = \frac{R_s}{b\eta} \cdot \frac{1 + \frac{2b}{a} \cdot \left(\frac{k_c}{k}\right)^2}{\sqrt{1 - \left(\frac{k_c}{k}\right)^2}} \left(\frac{NP}{m}\right) \tag{8}$$

where $a\&b$ are the aperture dimensions. R_s (mho/m) is the wall surface resistivity, and $\eta = 377\sqrt{\mu_r/\varepsilon_r}$ (ohm) is the propagation medium intrinsic impedance. It is evident that for the waveguides with low resistivity in actual cases, $\alpha_c(k)$ is small. Hence the exponential component due to damping in Eq. (5) is neglected. In this manner and using Eq. (6), a simpler form of Eq. (5) is written

$$E_s^{wgd}(k, r') = \hat{A}(r') \exp\left(-j2d\sqrt{k^2 - k_c^2}\right); \quad k > k_c \tag{9}$$

where $\hat{A}(r') = \Gamma(r')E_0$ is the weighting coefficient. Parameter d is called "dispersion length", and it is related to the waveguide physical length. The above weighting coefficient and the corresponding phase function represent the required amplitude and phase in Eq. (2). Thus, Eq. (3) becomes the parametric dispersive scattering centre model as

$$E_s^{DSC}(k) \approx \sum_{m=1}^{M} A_m \exp\left(-j2k\left(r_m + d_m\sqrt{1 - (k_{cm}/k)^2}\right)\right) \tag{10}$$

Here, the unknown parameters are $\{A_m, r_m, d_m, k_{cm}\}$; $m = 1, \ldots, M$. Hence, it is required to use a suitable optimization routine to calculate these four arrays of length M. The goal is minimization of the following fitness function over the measured coherent backscattered samples $(X_n;\ n = 1, \ldots, L)$ using a population based method [8]

$$S(A, r, d, k_c) = \sum_{n=1}^{L} \left|X_n - E_s^{DSC}(k)\right|^2 \tag{11}$$

Here, The general-purpose genetic algorithm MATLAB toolbox is used, but any other optimization techniques could be used. Due to existence of many local minima, care should be taken in the selection of the initial values for the unknown parameter. Selection of M is highly application dependent, and it cannot exceed $L/2$. The factors that should be considered include complexity of the dispersive geometry, sampling conditions (bandwidth, signal-to-noise ratio, etc.) and range resolution. Super-resolution methods can be used for initialization of $\{A_m\}$ and $\{r_m\}$. The initial guess for $\{d_m\}$ must be in the order of the waveguide physical length. The initial waveguide cut-off frequency $\{k_{cm}\}$ is the start of the frequency bandwidth. More detail about the above algorithm is explained in [14]. After determining the unknown parameters, the nonlinear group delay is represented by

$$\tau_{dm}^{nl} \approx -\frac{2}{c}\left(r_m + \varepsilon_m(k)\right) \text{ (sec)}; \quad \varepsilon_m(k) = d_m\sqrt{1 - (k_{cm}/k)^2} \text{ (m)} \tag{12}$$

where $\varepsilon_m(k)$ represents the frequency dependent spatial displacement. In radar range profiles, it is believed that this factor causes the range extension. The dynamic behaviour of aforementioned parametric group delay represents the range extension. It is also considered as a useful criterion for measuring the level of dispersion in nearby scattering centres. Due to using super-resolution techniques in our proposed parametric EDSC model (10), discrimination of DSCs with a high spatial resolution is possible. It is described in the next section.

4. EXPERIMENTAL RESULTS

In order to evaluate the effectiveness of the above proposed analysis method, it is implemented on a metallic geometrical model as a complex target that is excited in X-band. Here, due to finite size of aperture, excitation power limitations due to experimental instrumentation and margins of vector data sampling procedure in wide frequency range, small aspect angles are selected. In this manner, we are sure to have enough wave penetration inside the waveguide to observe the dispersion effect in the overall target scattering response. A linearly polarized plane wave illuminates the aperture side at $\theta \approx 45^{\circ}$. It is made of aluminium with 3 mm thickness and shown in Figure 3. This basic complex target is a combination of one 40 cm long open ended waveguide with aperture size of 2.7 cm $\times$ 2.7 cm and an 8 cm $\times$ 8 cm flat plate at the middle.

The measurement setup block diagram is shown in Figure 4. We use Rohde & Schwartz-ZVK VNA with 20 dBm output power which is fed to the double-ridged horn antenna with 22 dB gain at 9 GHz. The signal is transmitted toward the complex target placed on the Teflon table at 6.5 m away from the horn. The reflected wave is observed in time domain using VNA.

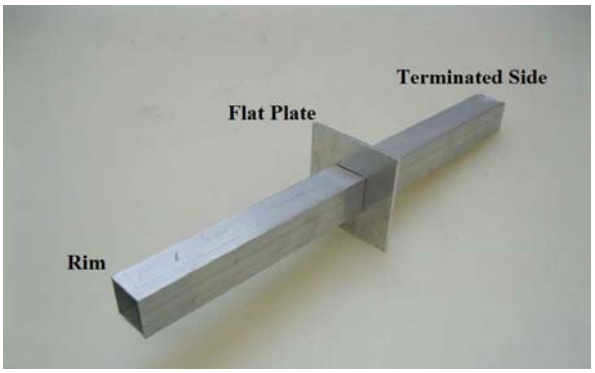

Figure 3. The geometrical model of the complex target for data sampling.

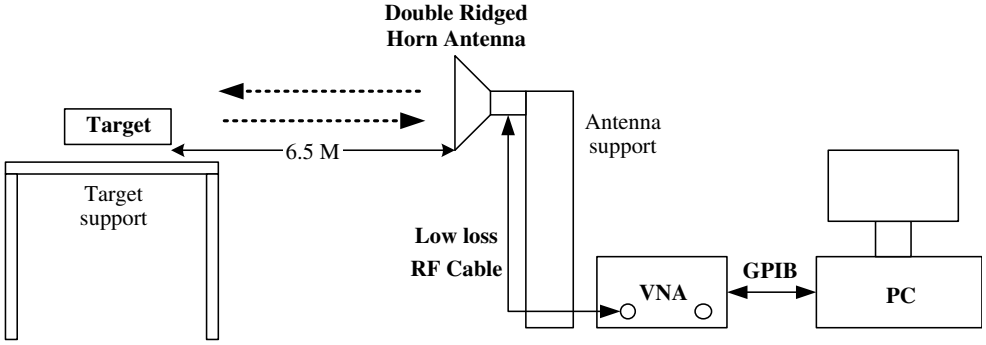

Figure 4. The block-diagram of measurement set up used for test.

It is predicted to have diffraction and/or reflection scattering mechanisms from the rim and flat plate geometrical discontinuities. Waveguide dispersion mechanism also exists due to wave penetration effect and relatively low aspect angle.

Hence, the backscattering from the rim, flat plate and outer surface of the terminated side make the non-dispersive scatterers. However, the round-trip radiated field from the aperture acts as the dispersive one. The determined range profile by parametric model (10) in 1 GHz frequency excitation bandwidth from 8 GHz to 9 GHz using 100 data samples is shown in Figure 5, and it is compared with IFFT outcome.

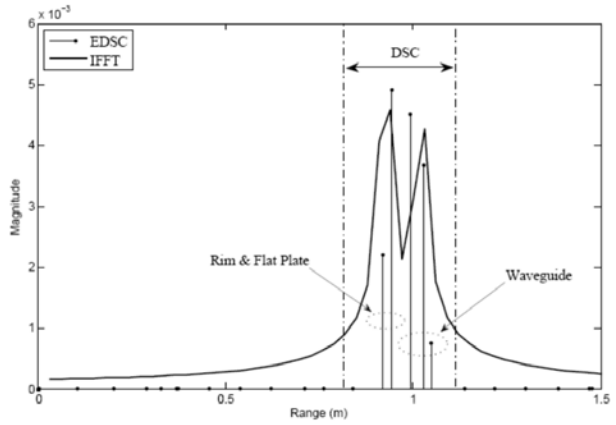

Figure 5. The range profile for 1 GHz bandwidth and 100 measured data samples.

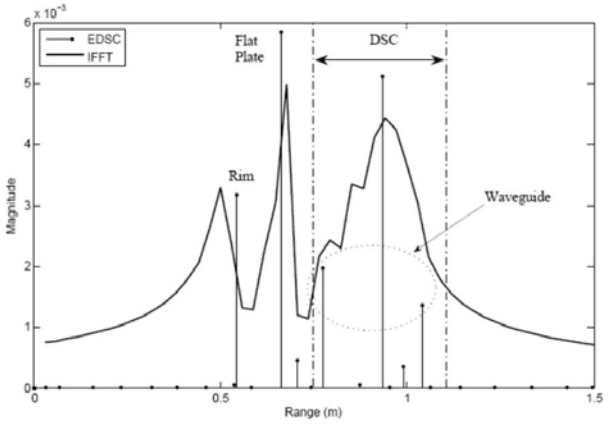

Figure 6. The range profile for 4 GHz bandwidth and 100 measured data samples.

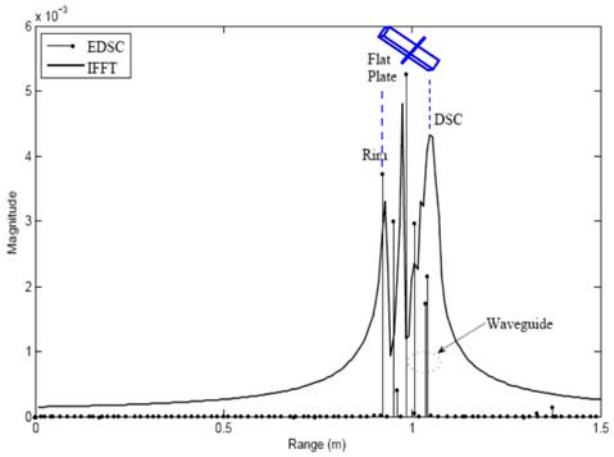

Figure 7. The range profile for 4 GHz bandwidth and 400 measured data samples.

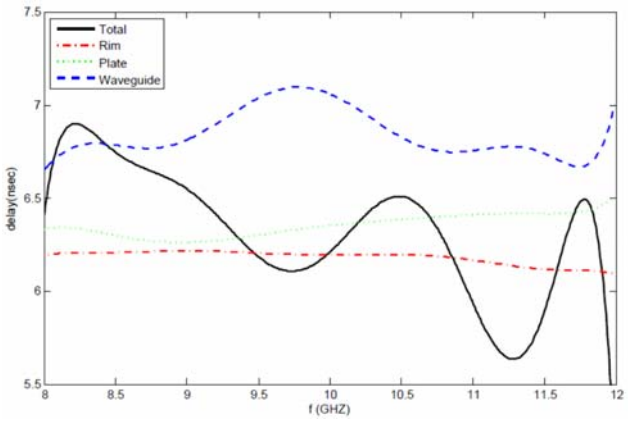

Figure 8. Comparison of total group delay in the complex target with individual identified scattering centres.

Our proposed method based on EDSC parametric model detects about five different scattering centres using finite data samples. However, at similar conditions, IFFT detects only two scatterers that are tightly combined to each other. Next, the bandwidth is increased to 4 GHz from 8 GHz to 12 GHz, and 400 data samples are measured in 10 MHz frequency steps. However, only 100 samples are picked up in this case which is in correspondence with the previous sparser 40 MHz frequency steps. The result is shown in Figure 6. By using such scaling, the resulted radar down range axis remains fixed with respect to Figure 5, and point to point comparison is possible.

As shown in Figure 6, again five dominant scattering centres are reported by our parametric method corresponding to the rim, middle flat plate and the waveguide. The first and second are single non-DSCs. The third one is a DSC consisting of at least three dominant jointed scatterers. However, the IFFT method only detects three main scattering centres with no further information about the corresponding scattering mechanisms. By synthesizing the phase of the individual scatterers, massive dispersion or group delay information is derived. It is performed by our proposed DSC analysis method described in previous sections. For this purpose, consider the original 400 data samples again. The corresponding range profile in this case is plotted in Figure 7.

Here, the original three main identified scattering centres are analyzed individually in order to measure the level of dispersive phase nonlinearity, i.e., group delay. For this purpose, each of them is

picked up using a definite range gate window. Then for each of the resulted gated scattering centres along the total range profile, two data arrays including a pair of scattering phase and amplitude are available. Performing the DSC analysis over each pair gives an individual group delay curve. The total group delay curve corresponding to the complex target and the individual discriminated scattering centres are sketched in Figure 8.

The rim and flat plate contributors demonstrate lower ripple about 0.25 nsec causing negligible dispersion. However, the waveguide contributor demonstrates higher group delay ripple level about 0.42 nsec. Hence, more effectiveness on total target group delay is expected due to waveguide dispersion. It is concluded that jointed scattering centres with a definite group delay ripple, with respect to a non-dispersive geometrical reference, is accounted for a waveguide type DSC. The analysis results are summarized in Table 1.

Table 1. Summary of the group delay analysis.

Geometrical discontinuity	Group Delay Ripple (nsec)	Jointed Scattering Centres	Waveguide Type Dispersion
Rim	< 0.25	1	Non-dispersive
Flat Plate	< 0.25	1	Non-dispersive
Waveguide	0.42	3	Dispersive
Total	1.25	-	Dispersive

5. CONCLUSION

Using a relatively simple parametric scattering model, an efficient technique is introduced to analyze the DSCs in complex targets. Based on measured data samples, group delay analysis is used as a criterion for discriminating the dispersive nature of the scatterers.

The spatial resolution of Fourier-based methods is bandwidth dependent. However, our proposed method uses super-resolution PRONY technique that yields satisfied resolution even for relatively narrower bandwidths and finite number of sampled data. It is used in complex range profile analysis including both of scattering phase and intensity [15]. Hence, more information about the target geometries is yielded in comparison with simple intensity range profiles. In realistic aerial targets, differentiating the waveguide type DSCs (engine intake, exhaust outlet) from non-DSCs (wings and tail) has significant applications in target identification methods. On the other hand, the technique introduced in this paper may be developed to be used to discriminate the DSCs in order to reduce their unwanted effects, such as reducing the smudge effects due to inlets/outlets in aerial targets in 2-D radar imaging. The important issue not included in this paper is noise. PRONY technique is susceptible to noise. Hence, replacing this super-resolution engine with a more efficient algorithm as Modified PRONY Estimator [16] or MPM [17] is recommended.

REFERENCES

1. Miller, E. K., "Model-based parameter estimation in electromagnetics: Part I. Background and theoretical development," *IEEE Antennas and Propagation Magazine*, Vol. 40, No. 1, 42–52, Feb. 1998.
2. Miller, E. K., "Model-based parameter estimation in electromagnetics: Part II. Applications to EM observables," *IEEE Antennas and Propagation Magazine*, Vol. 40, No. 2, 51–65, Apr. 1998.
3. Miller, E. K., "Model-based parameter estimation in electromagnetics: Part III. Applications to EM integral equations," *IEEE Antennas and Propagation Magazine*, Vol. 40, No. 3, 49–66, Jun. 1998.
4. Hurst, M. P. and R. Mittra, "Scattering centre analysis via Prony's method," *IEEE Trans. Antennas Propag.*, Vol. 35, 986–988, Aug. 1987.

5. Potter, L. C., D.-M. Chiang, R. Carriere, and M. J. Gerry, "A GTD-based parametric model for radar scattering," *IEEE Trans. Antennas Propag.*, Vol. 43, 1058–1067, Oct. 1995.
6. Trintinalia, L. C. and H. Ling, "Superresolved time-frequency parametrization of electromagnetic scattering mechanisms due to structural dispersion," *Microwave and Optical Technology Letters*, Vol. 10, No. 2, Oct. 1995.
7. McClure, M., R. C. Qiu, and L. Carin, "On the superresolution identification of observables from swept-frequency scattering data," *IEEE Trans. Antennas Propag.*, Vol. 45, No. 4, 631–641, Apr. 1997.
8. Heidar, H. and A. Tavakoli, "Highly dispersive scattering centre analysis using an enhanced parametric model," *IET Radar, Sonar & Navigation*, Vol. 5, No. 8, 895–901, Oct. 2011.
9. Moore, J. and H. Ling, "Super-resolved time-frequency analysis of wideband backscattered data," *IEEE Trans. Antennas Propag.*, Vol. 43, No. 6, 623–626, Jun. 1995.
10. Zhou, J., H. Zhao, Z. Shi, and Q. Fu, "Global scattering centre centre model extraction of radar targets based on wideband measurements," *IEEE Trans. Antennas Propag.*, Vol. 56, No. 7, 2051–2060, Jul. 2008.
11. Heidar, H. and A. Tavakoli, "Analysis of the radar range extension in open-ended waveguide type geometries," *IEICE Electronics Express*, Vol. 8, No. 9, 663–669, May 2011.
12. Burkholder, R. J. and P. H. Pathak, "Analysis of EM penetration into and scattering by electrically large open waveguide cavities using Gaussian beam shooting," *Proc. IEEE*, Vol. 79, No. 10, Oct. 1991
13. Rizzi, P. A., *Microwave Engineering Passive Circuits*, Prentice-Hall, 1988.
14. Heidar, H. and A. Tavakoli, "Wideband dispersion analysis of waveguide geometries using finite sampled data," *Progress In Electromagnetics Research M*, Vol. 16, 235–244, 2011.
15. Rihaczek, A. W. and S. J. Hershkowitz, *Theory and Practice of Radar Target Identification*, Artech House, 2000.
16. Carriere, R. and R. Moses, "High resolution radar target modeling using a modified prony estimator," *IEEE Trans. Antennas Propag.*, Vol. 40, No. 1, 13–18, Jan. 1992.
17. Sarkar, T. K., D. D. Weiner, and V. K. Jain, "Some mathematical considerations in dealing with the inverse problem," *IEEE Trans. Antennas Propag.*, Vol. 19, No. 4, 373–379, Mar. 1981.